Application of Multipolar Charge Models and Molecular Dynamics Simulations to Study Stark Shifts in Inhomogeneous Electric Fields†

Michael Devereux,* Nuria Plattner, and Markus Meuwly

Department of Chemistry, University of Basel, Klingelbergstrasse 80, 4056 Basel, Switzerland

Received: April 29, 2009; Revised Manuscript Received: July 2, 2009

Atomic multipole moments are used to investigate vibrational frequency shifts of CO and H_2 in uniform and inhomogeneous electric fields using ab initio calculations and Molecular Dynamics (MD) simulations. The importance of using atomic multipole moments that can accurately represent both molecular electrostatics and the vibrational response of the molecule to changes in the local electric field is highlighted. The vibrational response of CO to applied uniform and inhomogeneous electric fields is examined using Density Functional Theory calculations for a range of test fields, and the results are used to assess the performance of different atomic multipole models. In uniform fields, the calculated Stark tuning rates of $\Delta\mu = 0.52$ cm^{-1}/(MV/cm) (DFT), $\Delta\mu = 0.55$ cm^{-1}/(MV/cm) (fluctuating three-point charge model), and $\Delta\mu = 0.64$ cm^{-1}/(MV/cm) (Multipole model up to octupole), compare favorably with the experimentally measured value of 0.67 cm^{-1}/(MV/cm). For H_2, which has no permanent dipole moment, CCSD(T) calculations demonstrate the importance of bond-weakening effects in force fields in response to the applied inhomogeneous electric field. Finally, CO in hexagonal ice is considered as a test system to highlight the performance of selected multipolar models in MD simulations. The approach discussed here can be applied to calibrate a range of multipolar charge models for diatomic probes, with applications to interpret Stark spectroscopy measurements in protein active sites.

I. Introduction

Vibrational frequency shifts caused by external electric fields, often termed "Stark shifts", offer an increasingly important means to study the structure, electrostatics, and dynamics of protein active sites.[1,2] The response of bond vibrational frequencies to changes in local electric fields can be accurately measured and used to probe heterogeneous chemical environments. However, while detailed experimental data are available, it is difficult to model these processes within a theoretical framework. Ab initio calculations are too computationally expensive to adequately sample available phase space in large systems such as solvated proteins, and dynamics effects such as bond excitation are neglected when using "snapshot" sampling approaches. Classical force fields employed in many Molecular Dynamics (MD) simulations allow much more extensive sampling but may not be sufficiently detailed to provide realistic sampling of available space[3] or sufficiently sensitive to local changes in electric field to provide a realistic vibrational response. Use of more detailed, multipolar charge models offers one possible solution to provide a more accurate interaction with the inhomogeneous electric fields found in protein binding sites, while still allowing significant sampling of available phase space. If reliable theoretical data can be obtained, important additional information would be made available to aid interpretation of Stark spectroscopy measurements, linking observed vibrational frequency shifts to underlying structural and electrostatic features of the local chemical environment.

Vibrational frequency shifts in diatomic molecules or functional groups have been used to study molecular systems for some time.[4,5] For example, experimentally observed shifts in CO stretch frequency accompanying conformational changes in the active site of the protein myoglobin (Mb) have been used to explore protein structure and behavior.[6−8] Experimental measurements identified three distinct conformational substates of the binding site, based on splitting of the absorption peak of the CO ligand. The photodissociated molecule has been similarly studied[3,9,10] to reveal the motions and diffusion rates of free CO into different local pockets. The response of the CO stretch was again used to identify distinct local environments, this time corresponding to different positions around the binding site. Time-resolved spectroscopic measurements of ligand vibrational frequency in bound MbCO have also given a time scale for interconversion between bound conformational substates,[11] adding dynamical information to the structural and electrostatic data already available.

More recently, specially chosen diatomic functional groups with easily distinguishable infrared (IR) signals and strong vibrational sensitivity to local electric field strength have been attached to larger ligands and used to probe targeted regions of a protein active site. In this way, specific locations in a protein can be traced and the local electric field probed. The vibrational response of the probe group to an externally applied, uniform electric field can be easily measured to calibrate its behavior at different field strengths. When the probe is placed inside the protein environment, the induced vibrational frequency shift is compared to the known shifts at different uniform field strengths. One such experiment[2] measured the response of a nitrile substituent attached to a *h*ALR2 enzyme inhibitor in a series of fourteen *h*ALR2 mutants. The vibrational frequency of the calibrated nitrile probe was used to follow changes in the local electric field resulting from each mutation.

The Molecular Dynamics (MD) approach that accompanied these experiments to study substituent frequency shifts in the

† Part of the "Robert W. Field Festschrift".

* To whom correspondence should be addressed at michael.devereux@unibas.ch.

10.1021/jp903954t CCC: $40.75
Published on Web 08/14/2009

*h*ALR2 enzyme, however, followed only the evolution of the electric field strength at the probe position.[12] The calculated field strength at the molecular position was compared with experimental measurements of the frequency shift for each system. For a strong correlation to exist, it must be assumed that the behavior of the probe in the inhomogeneous field is roughly the same as that in an applied uniform field, i.e., the frequency will depend linearly on electric field strength, and there will be little deviation from this behavior arising from the field's inhomogeneous character. If the behavior is different, however, then the uniform field measurements used to calibrate the probe cannot be used to reliably infer the local electric field strength. A more detailed understanding of the interaction of the probe with the inhomogeneous field it encounters would then be required to interpret the measured vibrational frequency shift.

The evolution of the vibrational frequency of a probe in a molecular environment can alternatively be modeled in MD simulations directly via Fourier transform and the dipole−dipole autocorrelation function.[13] Dynamic effects are then incorporated, and the interaction with an inhomogeneous electric field, including higher field derivatives, can be more completely described. Following electric field evolution is often simpler than trying to model bond vibrational responses directly, however, as a detailed charge model for the probe substituent is not required. It has recently been demonstrated that atomic multipole moments up to quadrupole or octupole can be necessary in MD simulations to yield realistic atomic motions and responsive vibrational frequencies of small ligands or molecules within a protein binding site.[3] In these studies, detailed multipole representations were successfully applied to recover experimental vibrational spectra of photodissociated CO in myoglobin. Furthermore, it was subsequently shown that the same representation successfully captures the spectroscopic properties of CO not only in Mb but also in amorphous ices where the split lines are red- and blue-shifted instead of two red-shifted lines in Mb.[14] There are an essentially infinite number of ways, however, that a continuous molecular charge distribution can be divided into atomic contributions. This can be seen in the difference between atomic multipole moments obtained by partitioning a molecular wave function within the formalism of Bader's "Atoms in Molecules",[15,16] and those obtained using Stone's "Distributed Multipole Analysis".[17] Both methods accurately represent molecular electrostatics, but the different atomic multipole moments are likely to lead to somewhat different intramolecular forces when the molecule encounters an electric field. It is the aim of this study to compare the performance of point charge and multipolar force field models in realistically describing vibrational frequency shifts in MD simulations and to assess the impact of using different combinations of atomic multipole moments. A scheme is introduced that can be used to assess the performance of a given set of atomic multipole moments and can be incorporated into a fitting environment to refine initial multipole moments and improve performance of a charge model.

II. Theoretical Background

Vibrational Stark shifts, the response of bond vibrational frequencies to an applied uniform electric field, have been studied for many years. Quantum chemical treatment typically expresses the Hamiltonian as the sum of an unperturbed Hamiltonian and a response arising from interaction between the molecular dipole moment and uniform electric field:[5,18,19]

$$\boldsymbol{H} = \boldsymbol{H_0} - \mu\boldsymbol{F} \tag{1}$$

Here, μ and $\boldsymbol{F}$ are the molecular dipole moment operator and the uniform electric field, respectively. The vibrational frequency shift can then be approximated as the sum of a linear and quadratic term[19,20] in

$$\Delta\bar{\nu}(\mathbf{F}_{||}) = -\frac{1}{hc}\left(\Delta\mu\cdot\mathbf{F}_{||} + \frac{1}{2}\mathbf{F}_{||}\cdot\Delta\alpha\cdot\mathbf{F}_{||} + \cdots\right) \tag{2}$$

where $\mathbf{F}_{||}$ is the uniform field component along the bond axis. $\Delta\mu$ and $\Delta\alpha$ are the "difference dipole moment" or "Stark tuning rate" and "difference polarizability", respectively. These quantities differ from the more widely used expectation values of the molecular dipole moment and polarizability operators.

In order to apply the powerful tools of classical MD simulations to investigate vibrational frequency shifts, Boxer et al.[20] developed a formalism which divides the vibrational response into two contributions: "mechanical anharmonicity" and "electronic bond perturbations". Mechanical anharmonicity results from a combination of the anharmonicity of a bond energy profile as a function of bond length, and direct interaction of charge with the electric field. Electronic bond perturbation refers to the effect of charge polarization on bond strength, altering the bond energy profile. Within a force field, mechanical anharmonicity can be included by using an anharmonic (for example Morse) bonded potential, so that a vibrational frequency shift occurs due to interaction between the atomic charges and the electric field. The second component, electronic bond perturbation, amounts to alteration of the bond force constant or Morse parameters as a function of local electric field strength.

An important additional consideration, often neglected when describing Stark shifts in heterogeneous environments, is that vibrational response in a uniform and an inhomogeneous electric field differ. Many vibrational models have been created to describe experimental Stark spectroscopy data, which is traditionally measured using macroscopic equipment to generate a field that is essentially uniform to microscopic dimensions. Equation 2 is therefore strictly only applicable to uniform fields. For an inhomogeneous field the Hamiltonian should be extended to[21]

$$\boldsymbol{H} = \boldsymbol{H}_0 - \mu\boldsymbol{F} - \frac{1}{3}\Theta\boldsymbol{F'} - \ldots \tag{3}$$

where μ is the dipole moment operator and $\boldsymbol{\Theta}$ is the quadrupole moment operator. The fields generated by a realistic charge distribution in a protein, for example, and by point charges in force field descriptions, contain higher field derivatives and therefore cannot be considered as uniform. This approximation is only realistic for probe molecules at large distances from the field-generating charges. The electrostatic interaction energy of a charge distribution with an inhomogeneous electric field can be described after expanding the charge distribution as a multipole expansion and summing the contribution of each term according to[22]

$$V_{\mathrm{elec}} = qV(\mathbf{r}) - \mu_\alpha F_\alpha - \frac{1}{3}\Theta_{\alpha\beta}F'_{\alpha\beta} - \ldots \tag{4}$$

Here V_{elec} is the total electrostatic interaction energy of the charge distribution with the inhomogeneous field. q is the charge term of the multipole expansion. $V(\mathbf{r})$ represents the electrostatic potential energy generated by the electric field at the position of the spatial origin of the multipole expansion $\mathbf{r}$. F_α is the α

component of the electric field, $F_\alpha = -\partial V/\partial r_\alpha$. $F'_{\alpha\beta}$ is the $\alpha\beta$ component of the field gradient $F'_{\alpha\beta} = -\partial^2 V/\partial r_\alpha \partial r_\beta$. In a uniform electric field the field gradient and higher derivatives are all zero, so that only the charge and dipole moment contribute to the interaction energy. In inhomogeneous electric fields, higher derivatives may contribute as well. For long-range interactions the field strength dominates the higher derivatives, so the uniform field approximation is likely to be applicable. For short-range interactions, the higher derivatives of the electric field will interact more strongly with the multipole moments of the bonded atoms, and the vibrational shift may deviate from the predictions made by calibrating a molecule in a uniform field.

Interactions between a molecule and an external electric field can be investigated using rigorous electronic structure or more approximate force field methods. For a diatomic molecule, a complete force field representation consists of bonded and nonbonded terms. This is different from a full quantum mechanical treatment which does not decompose the interactions but explicitly treats interactions between all protons, electrons, and external forces of the system simultaneously. To capture fine details of the interaction between a diatomic molecule and its environment using force fields, the decomposition into internal (bonded) and external (nonbonded) terms may lead to inaccuracies. In a force field the bonded terms are not perturbed by the external field and the vibrational response results from the nonbonded interactions which are partitioned into largely arbitrarily localized atomic contributions and result from the charges assigned to each atom. The charge model used is therefore important for obtaining realistic vibrational shifts. Multipolar force fields offer the potential to more accurately describe the molecular electrostatic interaction energy and to better control division of the total energy between atoms. Such methods are becoming increasingly widespread,[3,23,24] as the more detailed descriptions of anisotropic charge distributions have led to higher levels of accuracy than was possible using point charge approaches.[25] At the same time they require significantly lower computational effort than full ab initio calculations. When using multipoles, however, a scheme must still be chosen to apportion components of the molecular charge density between individual atoms. The fact that different partitioning methods that accurately represent the same molecular charge density can still lead to different vibrational behavior must then be taken into account.

In order to capture additional effects such as the "electronic bond perturbations" described above, it might also be necessary to consider the bonded terms, and to allow them to respond directly to an external field. Such effects will be particularly important in systems where the number of electrons is small and where no permanent low-order multipole moments are present, e.g., H_2. For other systems, such as CO, these effects are smaller because most of the electron density remains unperturbed. Such aspects will be exemplified in the results section.

An additional point to keep in mind when investigating vibrations in MD simulations, is between realistic sampling and realistic vibrational behavior. Any multipolar model that accurately represents molecular multipole moments should lead to similar, accurate intermolecular interaction energies and therefore similar sampling of available phase space during an MD simulation. As already stated, accurate intermolecular interaction energies and sampling will not yield realistic vibrational behavior unless accompanied by a model that also gives a realistic vibrational response from the intramolecular forces experienced. Similarly, though, a model that gives a reasonable vibrational response to an applied field will not yield accurate vibrational behavior in an MD simulation if the intermolecular interaction energies are not accurate and the available phase space is not realistically explored.

III. Computational Methods

A. Ab Initio Calculations. The effects of an inhomogeneous electric field on the CO vibrational frequency were evaluated using B3LYP Density Functional Theory calculations[26,27] in the Gaussian03 suite of programs.[28] The CO molecule was treated using an aug-cc-pVQZ basis set, found to yield an accurate description of the experimentally measured molecular multipole moments at relatively low computational cost. Uniform electric field calculations were performed using the "Field" keyword to introduce a dipole electric field into the Hamiltonian of the Gaussian03 geometry optimization and energy calculations. A simple inhomogeneous field was created by replacing the dipole electric field with a negative point charge in the DFT calculation, placed at a selected position on the oxygen side of CO along the molecular axis. The magnitude of the point charge was chosen to create a desired field strength at the position of the CO center of mass. The distance from the center of mass could then be varied, while simultaneously altering the magnitude of the point charge to maintain the same electric field strength at the CO position as before. In this way the electric field strength could be kept constant while examining the effect of higher derivatives of the electric field on vibrational frequency. The strength of the field used throughout this study is 43 MV/cm, relatively strong for an applied uniform field but equivalent to a point charge of -0.27 au at 3 Å separation, which is quite realistic in an MD simulation. The larger shifts created also allow clearer evaluation of the performance of the models. Results at 21.5 and 86 MV/cm reveal qualitatively very similar behavior, although the stronger 86 MV/cm field leads to shifts outside the linear regime and smaller than would be predicted by eq 2. Similar calculations were performed for H_2 using the same point charge arrangements in CCSD(T) calculations, again with an aug-cc-pVQZ basis set.

B. Charge Models. A variety of different CO electrostatic models were examined, including a number taken from previous Molecular Dynamics studies. The simplest—referred to as "point charges" in the following—used CHARMM22[29] gas phase charges of 0.021 and -0.021 au for C and O, respectively. A three-point fluctuating charge model previously used to model the vibrational spectra of photodissociated CO in myoglobin[10] (Mb) was also tested. The model employs fitted charges positioned at the C and O nuclear positions, with an additional charge site at the CO center of mass (COM) to yield accurate molecular multipole moments up to quadrupole. Charges fluctuate as a function of bond length to encapsulate intramolecular charge polarization, according to

$$q_C = -10.5 + 19.1r - 12.3r^2 + 2.9r^3 \qquad (5)$$

$$q_O = -9.8 + 18.9r - 13.4r^2 + 3.4r^3$$

$$q_{COM} = -(q_C + q_O)$$

In addition, models based on atomic multipole moments from a Distributed Multipole Analysis using the GDMA program,[30] were tested. These models have again been successful to study vibrational spectra of photodissociated CO in Mb.[3] The models

TABLE 1: Multipolar Charge Models Used To Describe Electrostatic Interaction with an External Electric Field

	atom	model A	model B	model C	model C′	AIM
charge [e]	C	−0.5639 [0.5128]	0.2703 [0.2275]	0.5634 [0.1246]	0.3466 [0.0739]	1.1749 [−0.5368]
dipole [ea_0]	C	−0.2262 [−0.5819]	0.8181 [−0.4316]	1.0962 [−0.3952]	0.8810 [−0.1515]	1.6490 [−0.5522]
	O	−0.9558 [0.3900]	−0.1803 [0.5183]	0.1343 [0.5133]	−0.1044 [0.1775]	0.8939 [−0.1533] [−0.8259]
quadrupole [ea_0^2]	C			−0.0507 [0.0871]	−0.0367 [−0.0283]	0.0641 [0.8895]
	O		0.5621 [−0.3242]	0.4672 [−0.4534]	0.6244 [−0.0879]	0.05487 [−0.2902] [0.9730]
octupole [ea_0^3]	C				0.1992 [0.1974]	−1.0399 [1.3982]
	O			−1.7748 [0.6641]	−1.2398 [−0.0489]	−1.8856 [1.3644]
Lebedev radii [Å]	C	0.500	0.660	0.700	0.800	N/A
	O	0.770	0.600	0.525	0.700	N/A

differ in the atomic radii used for the Lebedev integration in GDMA and also in the maximum atomic multipolar rank included (Table 1).

Finally, a new multipolar model was developed by calculating atomic multipole moments at the B3LYP/aug-cc-pVDZ level of theory using the "Atoms in Molecules"[15,16] partitioning method. Atomic multipole moments up to octupole were evaluated using the MORPHY98 program[31] as a function of bond length, and linear or quadratic functions were fitted to describe the variation.

Two similar multipolar models were fitted for H_2 at the B3LYP aug-cc-pVQZ level of theory, one using AIM multipole moments and one using DMA. The B3LYP density was used in place of CCSD(T) to obtain a description of the electron density for the AIM and DMA partitioning software. The more approximate representation of the density used to fit the charge models is not expected to significantly affect results.

C. Vibrational Frequency Calculations. DFT vibrational frequency calculations were performed by stretching and compressing the CO bond at 0.025 Å intervals around the equilibrium (geometry-optimized) bond length. The energies obtained were fitted to a Morse potential and the LEVEL[32] program was used to obtain the ground and first excited vibrational energies from which the frequency shift $\Delta\nu$ was calculated. The same method was used for H_2 vibrational frequency calculations at the CCSD(T)/aug-cc-pVQZ level of theory.

Vibrational frequencies were obtained for the various charge models using a similar approach. Morse parameters fitted from sampling the CO bond length in DFT calculations in the absence of an applied electric field were used to describe the bonded energy in the molecular mechanics calculations. An additional nonbonded energy was added to describe electrostatic interaction between the molecular charge density and the applied electric field. The total energy (bonded + nonbonded) was sampled at 0.025 Å intervals as before, a new Morse potential was fitted, and LEVEL was again used to obtain $\Delta\nu$. In this way calculated DFT and molecular mechanics vibrational frequencies can be directly compared, which allows the performance of different charge models to be evaluated. More direct comparison with DFT results for atomistic simulations is difficult, due to the computational cost required to obtain statistically meaningful sampling of phase space using ab initio calculations.

D. Randomly Generated Field Calculations. The situation in a heterogeneous environment was emulated by creating 30 inhomogeneous electric fields by placing 500 point charges at random positions inside a 40 Å × 40 Å × 40 Å box (Figure 3). The fields differed by the partial charges used: 10 fields included randomly assigned point charges with charges anywhere between −0.65 and 0.65 au, 10 fields used random charges between −0.65 and 0.55 au (bias toward increased negative charge in the box), and 10 fields used charges between −0.55 and 0.65 au (bias toward increased positive charge). The CO molecule was placed at the center of the box, and no point charges were placed within 2 Å of the molecular center of mass. Ab initio calculations were performed in combination with the LEVEL program (as described above) to determine the vibrational frequency of CO or H_2 in each field. The different MD charge models were then tested by using LEVEL to evaluate the vibrational frequency associated with each model in each field, and comparing to DFT results.

E. MD Simulations of CO in Ice. The setup for CO in ice follows closely previous simulations,[14] except that here all simulations were carried out with the TIP3P water model.[33] This water model is suitable for testing the frequency shifts obtained with different CO models but should be replaced for more quantitative studies. A hexagonal ice structure composed of 1024 water molecules with dimensions 35 × 31 × 29 Å was taken as a starting structure and a CO molecule was inserted either between the water molecules (interstitial) or replacing a water molecule (structural). All simulations were carried out with the CHARMM program.[34] The structures were first optimized and equilibrated for 20 ps at 20 K. Then production runs for the spectra of 100 ps at 20 K in the *NVT* ensemble followed using Berendsen's weak coupling method.[35] A time step of 1 fs was used, and the O−H bonds were constrained using the SHAKE algorithm.[36] For CO, four electrostatic models were compared, namely, simple point charges, Model C and Model C′ of Table 1, and the atoms in molecules (AIM) model in Table 1. For the CO bond, the RRKR potential was used.[37,38] The gas phase CO frequency is found at 2187 cm^{-1} at 20 K for this potential and a time step of 1 fs.[14]

The infrared (IR) spectrum is calculated from the Fourier transform of the dipole moment autocorrelation function $C(t)$ which is accumulated over 2^n time origins, where n is an integer such that 2^n corresponds to between 1/3 and 1/2 of the trajectory, with the time origins separated by 1 fs. $C(t)$ is then transformed to yield $C(\omega)$ using a fast Fourier transform with a Blackman filter to minimize noise.[39] The final classical infrared absorption spectrum $A(\omega)$ is then calculated from

$$A(\omega) = \omega\{1 - \exp[-\hbar\omega/(kT)]\}C(\omega) \qquad (6)$$

where k is the Boltzmann constant and T is the temperature in Kelvin.

IV. Results

A. Deviation from Uniform Electric Field Behavior. First, results from DFT calculations to assess the effects of inhomogeneous vs uniform electric fields on the vibrational response are considered. The top half of Figure 1 shows the effect of approaching a point charge from 100 to 3 Å along the CO bond vector, while adjusting the magnitude of the charge to maintain a constant electric field strength (see "Methods" section). As the point charge approaches the CO center of mass, the higher

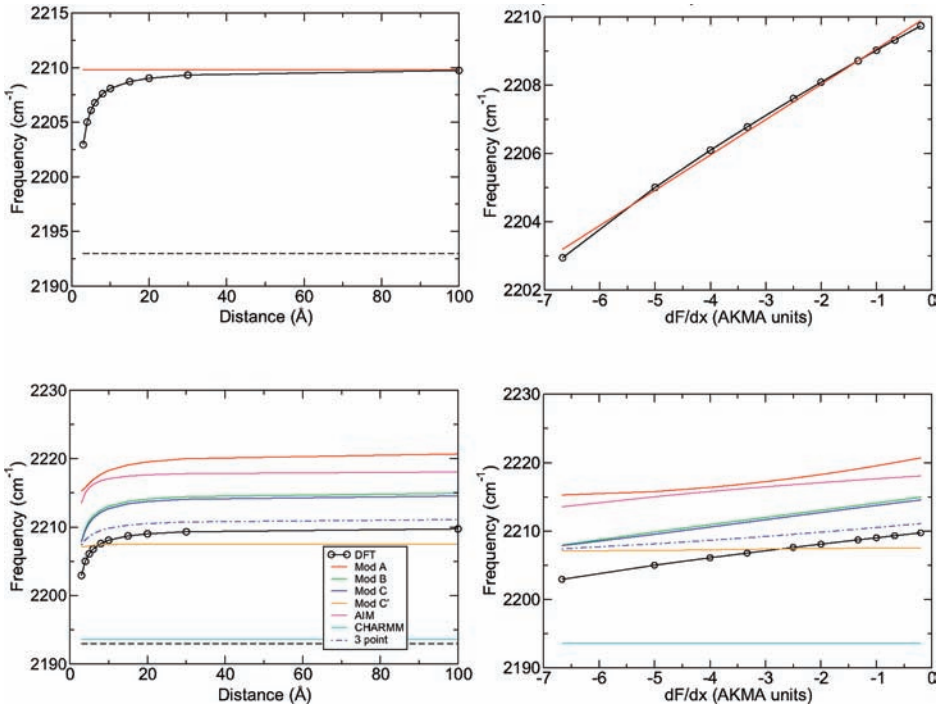

Figure 1. (Top left) Black: DFT vibrational frequency of CO as a function of distance from the point charge used to apply an inhomogeneous electric field with dipole component 43 MV/cm (see text for details). Dashed: Vibrational frequency in the absence of an external electric field. Red: DFT vibrational frequency shift after applying a uniform electric field. (Top right) Black: CO DFT vibrational frequency shift as a function of electric field gradient at constant electric field strength. Red: Linear regression fit. (Bottom left) Same as top left, now including the performance of the different charge models listed in the key with DFT results. (Bottom right) Plot of each model against the field gradient.

field derivatives, which decay more rapidly with the charge separation than the electric field strength, become more significant. The field originating from a large point charge at 100 Å therefore results in very small higher derivatives of the electric field at the CO position, and the frequency shift of 22.4 cm^{-1} is essentially identical to the result in a uniform field (shown in red) of 22.5 cm^{-1}. The shift of 22.5 cm^{-1} in the applied field of 43 MV/cm represents a Stark tuning rate of $\Delta\mu = 0.52$ cm^{-1}/(MV/cm), in reasonable agreement with the experimentally measured value of 0.67 cm^{-1}/(MV/cm)[40] when considering the differences between the fixed, gas phase calculation in a relatively strong applied field and the experimental setup of a free, dynamic CO molecule in a frozen solvent. As the point charge is moved closer, however, and the higher derivatives of the electric field become larger at the same field strength, there is strong deviation from the uniform field behavior. At 3 Å the frequency shift is only 13.7 cm^{-1}, just over half of the frequency shift in the uniform case. This result demonstrates that for CO, frequency shifts measured in inhomogeneous electric fields cannot be reliably approximated using results calculated or measured in a uniform field, and higher field derivatives must be taken into account.

The right-hand side of Figure 1 shows the deviation in vibrational frequency as a function of the first derivative of the electric field strength with respect to displacement along the molecular axis. The figure demonstrates that the relationship is essentially linear and the deviation from uniform field behavior is directly proportional to the first derivative of the electric field. This suggests that the deviation from the uniform field behavior is due primarily to interaction with the molecular quadrupole moment, which interacts with the electric field gradient according to eq 4. The relatively large effect of the quadrupole moment can be rationalized by considering the small molecular dipole moment of CO (0.048 ea_0), and the more substantial quadrupole moment (-1.58 ea_0^2).[41−44]

The bottom half of Figure 1 shows the performance of the different multipolar charge models (see Methods and Table 1 for details) in the same point charge arrangement. All models yield accurate molecular electrostatics up to quadrupole moment, with models B, C, and C′, as well as the new model fitted from Atoms in Molecules calculations (model AIM) additionally yielding molecular octupole moments in reasonable agreement with previously reported values.[41,42] It can be seen that models B and C perform similarly to one another and give results close to DFT values. The magnitude of the shift in a uniform field, approximated here by a large point charge placed at long-range, is overestimated by around 5 cm^{-1}, but the interaction with higher field derivatives is quite accurate, as shown by the similar gradients in Figure 1. Model AIM also performs well, although the shift due to interaction with the dipole field component is larger at around 8 cm^{-1} above the DFT value. Model C′ leads to a more accurate interaction with the dipole field component but poor interaction with higher electric field derivatives, as highlighted in Figure 1. Model A leads to the poorest overall behavior, significantly overestimating interaction with the dipole electric field component and not displaying a linear response to the electric field gradient. This is likely to be a result of the lack of higher atomic multipole moments on the C and O atoms in this model (Table 1). The vibrational frequency shift using only point charges is extremely small in the dipole field and does not noticeably interact with higher derivatives of the electric field. This is a result of the very small charges that are used (0.021 and -0.021 au), required to maintain a realistic molecular charge and dipole moment in the absence of higher atomic multipole moments. This point charge model, which is typically designed to achieve realistic nonbonded interaction energies, is not suitable for modeling vibrational frequency shifts in an electric field. Perhaps surprisingly, however, the three-point fluctuating charge model yields a very accurate response to the dipole field component, and hence a realistic Stark shift

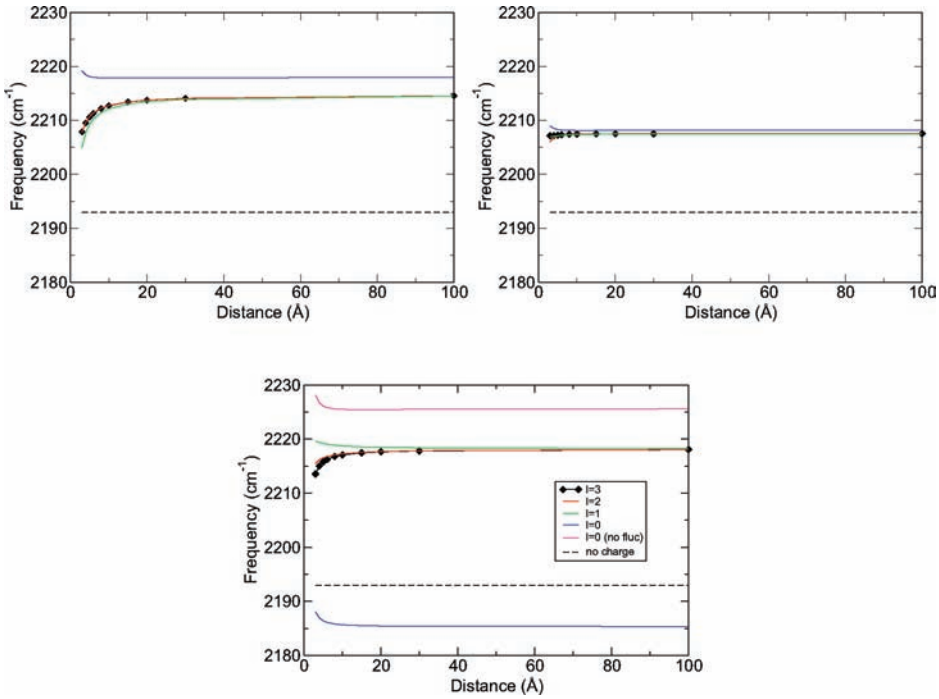

Figure 2. Convergence of model C (top left), model C′ (top right), and model AIM (bottom) after sequentially increasing the highest atomic multipolar rank from $l = 0$ to $l = 3$. Model AIM includes an additional curve with static (nonfluctuating) atomic charges. Colors correspond to the key included in the bottom chart.

in response to the distant point charge. The vibrational interaction with higher derivatives of the electric field (Figure 1) is less accurate than models B, C, and AIM, but more accurate than model C′. It should be noted, however, that the three-point fluctuating charge model only leads to accurate molecular multipole moments up to quadrupole, meaning that total molecular interaction energies are less accurate than models with atomic multipole moments up to rank $l = 3$.

B. Convergence of the Multipolar Models. One explanation for the different behavior of the multipolar models in the inhomogeneous electric field is convergence of the multipole-field interaction with the rank of the atomic multipole expansion. Previous studies have shown this convergence behavior to be an important consideration when using multipolar models.[3,45,46] Figure 2 shows the convergence of Models C, C′, and AIM by incrementally increasing the maximum atomic multipolar rank. Figure 2 demonstrates that Models C and C′ both approach convergence at rank $l = 1$ (with fluctuating charges and dipole moments on both atoms) and appear essentially fully converged even when significant higher electric field derivatives (demonstrating a strongly inhomogeneous field) are present by $l = 2$. All models converge in their interaction with the dipole component of the electric field by rank $l = 1$. This is expected when considering eq 4, as no moments higher than dipole interact with a homogeneous electric field.

The AIM model (bottom of Figure 2) converges more slowly, a result previously reported in comparing electrostatic interaction energies from AIM and DMA expansions.[45] An alternative scheme devised within the AIM framework to distribute atomic multipolar origins away from the atomic nuclear position may improve convergence,[47] although it would be more difficult to implement computationally. The model has nearly converged by $l = 2$, however, and provides good agreement with DFT results for interaction with higher derivatives of an electric field by $l = 3$ (Figure 1). The very poor behavior with $l = 0$ at first appears counterintuitive, as the large positive charge on C and negative charge on O at equilibrium bond length (Table 1) are expected to interact with the dipole electric field component to provide a reasonably large blue shift, rather than the small red shift that is observed in Figure 2. Indeed, this is the case when static charges of this magnitude are applied, also shown in the figure. The red shift is actually due to the large charge fluctuation on both atoms as a function of CO bond length. This fluctuation is opposite to that of models A, B, C, and C′, as the magnitude of the atomic charges decreases with increasing bond length. The result is that while an increase in stability (lowering of electrostatic interaction energy) is achieved by increasing bond length, moving O closer to the applied positive charge and C further away, the atomic charges are simultaneously decreased, thereby decreasing the stabilizing interaction by a greater amount. This effect is counteracted by adding the fluctuating dipole moment term to give more realistic behavior.

The fact that the interaction of all models with the applied inhomogeneous fields appears to have essentially converged by rank $l = 3$ suggests that their different behavior—especially when significant higher electric field derivatives are present—depends on the partitioning method used and not on convergence of the multipole expansion. The models compared in Figure 2 all have accurate molecular multipole moments up to octupole (see Methods section).

C. Performance of Charge Models in Randomly Generated Fields. So far, inhomogeneous fields have been generated by a single point charge, meaning that the gradient vector field of the electric field ∇F "fans out" from the position of the point charge. In a uniform field, gradient vector field lines of the electric field run parallel to one another. A single point charge placed at very long distance also has gradient vector field lines that run approximately parallel to one another, to the microscopic dimensions of a diatomic molecule. The following section describes the performance of different electrostatic charge models in yielding realistic vibrational shifts for CO in more heterogeneous electric fields, involving combinations of many point charges at different separations. This represents more closely a field encountered, e.g., in a protein binding site. Thirty

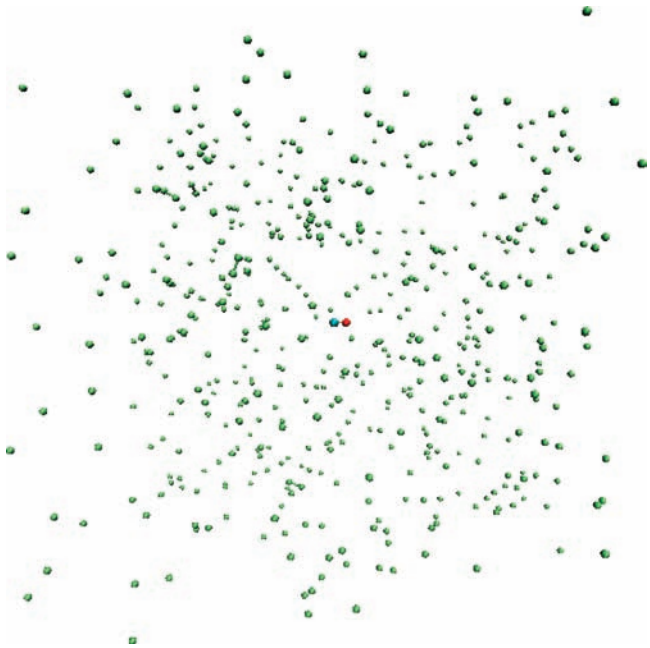

Figure 3. Example of an arrangement of randomly positioned point charges (green spheres) with randomly assigned charges used to generate a highly inhomogeneous electric field. The CO molecule is shown at the center of the arrangement.

randomly generated fields with arrangements such as that shown in Figure 3 were tested. The vibrational frequencies associated with each model are shown alongside the DFT vibrational frequency in Figures 4. Results are sorted by DFT vibrational frequency along the *x*-axis, with the electric fields assigned an integer index. The DFT reference values are shown as black diamonds and span a range of ≈100 cm^{-1}. It should be noted that the large shifts are the result of a particular "conformation" (arrangement), so are likely to be larger than typically observed experimental shifts that are averaged over many conformations. The dashed line shows the result of using no charge model (the zero field vibrational frequency of the force field Morse potential). All models other than simple point charges yield qualitatively reasonable results. Point charges are too small to yield a significant vibrational response.

Models A, B, C, and C′ exhibit similar vibrational behavior to one another, although models A and C′ have larger errors compared to DFT results than models B and C. The bottom part of Figure 4 shows that the mean absolute error (MAE) of model A is 7.4 cm^{-1}, while that of model C′ is 6.9 cm^{-1}, compared with 3.8 and 3.5 cm^{-1} for models B and C, respectively. The MAEs of models A and C′ become significant when compared to the mean absolute frequency shift of 19.1 cm^{-1}. The poorer behavior of model A could be attributed to inadequate representation of the molecular octupole; however model C′ contains a more detailed description of the molecular charge density than models B and C but still results in an inferior description of vibrational behavior. This result again demonstrates that while a chemically intuitive partitioning of the molecular charge density using an atomic multipole expansion yields good qualitative vibrational behavior in an applied, inhomogeneous electric field, small differences are introduced by the particular choice of partitioning method. The accuracy of these models to capture vibrational response also mirrors to some extent the performance of the models in yielding accurate CO vibrational spectra in MD simulations of photodissociated CO in Mb.[3] A larger factor in the MD results, however, is likely to be the less realistic sampling obtained by model A as a result

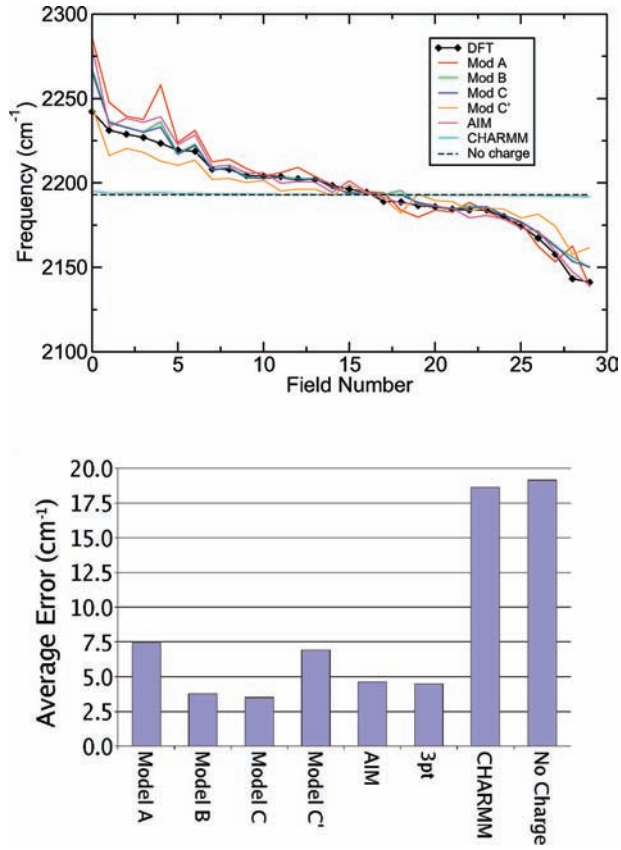

Figure 4. (Top) Vibrational frequency using different CO charge models in 30 randomly generated electric fields. Fields are sorted by decreasing vibrational frequency of DFT results. (Bottom) Mean absolute error in vibrational frequency for each charge model, taking DFT data as a reference.

of poorer description of the molecular octupole moment by neglecting higher atomic moments (see Methods and ref 3 for details).

The results obtained using model AIM lie between models B and C′, with an MAE of 4.6 cm^{-1}. The AIM results are affected by the fact that the atomic multipole moments are determined by the electron density contained within the finite and fixed atomic volume defined by the partitioning method. No parameters such as the integration radii as in DMA can therefore be used to obtain different atomic multipole moments that could be used to tune vibrational behavior. A final, perhaps surprising, result is the continued robustness of the three-point fluctuating charge model across a range of randomly generated fields. As shown in Figure 4, the MAE of 4.5 cm^{-1} places the model's performance approximately equal to that of model AIM, and better than models A and C′ in its representation of vibrational behavior. It appears, then, that the less accurate interaction with the higher electric field derivatives (Figure 1) is compensated by the more accurate interaction with the dipole field component to provide a model of good overall accuracy. The main reason for the improved performance of model C over the three-point charge model in modeling IR spectra in previous MD simulations in Mb[3] is therefore likely to be the more accurate higher multipole moments leading to more realistic sampling throughout a trajectory. The fluctuating charge approach may therefore offer a less computationally expensive means to model vibrational frequency shifts in classical MD simulations than use of a full multipole expansion, although sampling can be less accurate than the more detailed electrostatic approaches. The three-point model may also offer a more robust

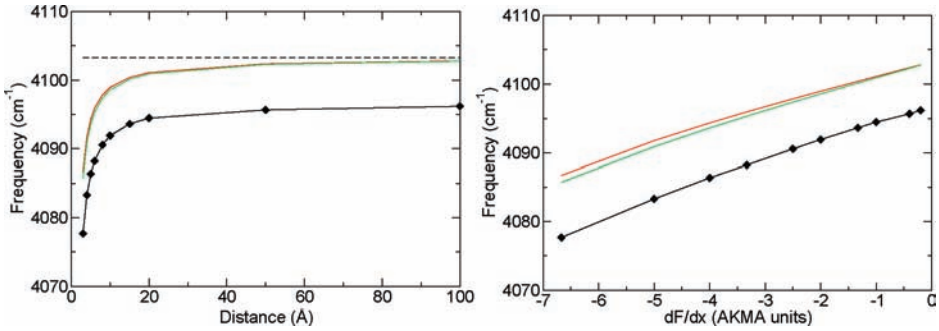

Figure 5. (Left) Black curve: Plot of H_2 CCSD(T) vibrational frequency shift as a function of distance between the point charge and H_2 center of mass. Dashed line: Plot of H_2 CCSD(T) vibrational frequency in the absence of an external electric field. Red curve: Results using a model with AIM atomic multipole moments up to octupole and green curve: results using a DMA model, also with atomic multipole moments up to octupole. (Right) Colors correspond to the first figure, the *x*-axis now represents the gradient of the electric field along the molecular axis.

alternative to use of a full multipole expansion, as the stability of large scale multipolar simulations as a function of the number and multipolar rank of interaction sites remains to be fully explored.

V. Vibrational Shifts for H_2

H_2 was chosen as an additional test system.[48,49] The symmetry of the molecule means that there are no molecular multipole moments of rank lower than quadrupole. The Stark shift in a uniform electric field is therefore predicted to be small due to the lack of a permanent molecular dipole moment. The behavior of H_2 in different applied fields, again of strength 43 MV/cm and with higher field derivatives adjusted by moving a single point charge as before, is shown in Figure 5. Despite the lack of a dipole moment, there is a calculated CCSD(T) red shift of around 7 cm^{-1} in the uniform electric field. Unlike a typical Stark shift, though, the same red shift is observed when the electric field direction is reversed. The shift is likely to arise primarily from weakening of the H_2 bond, as little polarization of the electron density was found to take place due to the low number of electrons in the system. Interaction energies between the polarized electron density of the H_2 molecule and an applied electric field were therefore found to be almost the same as between the field and the unpolarized density. More interestingly, a qualitatively similar interaction between the higher field derivatives and the molecular charge distribution arises as for CO (Figure 1). The total red shift with a point charge placed 3 Å from the H_2 COM is 25 cm^{-1}, much larger than the 7 cm^{-1} shift in a uniform field. The two multipolar charge models, one fitted using AIM atomic multipole moments and one using DMA, exhibit a quantitatively similar interaction with the higher field derivatives, and good agreement with the CCSD(T) behavior (as demonstrated by the similar gradients in the right-hand side of Figure 5). The systematic shift in vibrational frequency is due to the lack of a polarizable Morse potential in the force field model. There is therefore no bond weakening in the applied uniform electric field, and as there are no atomic charges, there is no resulting frequency shift.

The models have again been compared, this time with CCSD(T) results, in the same series of randomly generated electric fields as used for CO in Figure 4. As shown in Figure 6, the range of frequency shifts for H_2 in the randomly generated fields is around 70 cm^{-1}, significantly smaller than for CO in the same series of fields (Figure 4). The multipolar charge models do not perform as well as for CO, generally overestimating the vibrational frequency but not systematically. This overestimation is likely to be a result of the same effect that caused the systematic shift in Figure 5, i.e., the neglect of a bond-weakening term to alter the bond strength in response to the applied electric field. As a result, blue-shifted CCSD(T) data are better predicted than red-shifted data, as in blue-shifted data the interaction between higher multipole moments and the higher derivatives of the electric field is dominant. Where the bond weakening effect is large, however, significant errors are introduced by using the multipolar force field models. Explicit inclusion of bond weakening effects in force field calculations would require consideration of quantum mechanical terms associated with molecular charge polarization. It may be possible, however, to fit an expression to describe bond weakening as a function of applied electric field strength and orientation to approximate the missing terms.

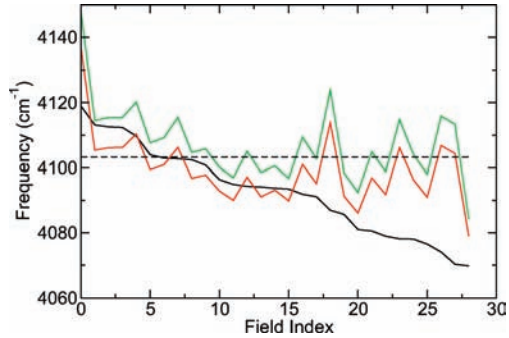

Figure 6. Vibrational frequency using different H_2 charge models in 29 randomly generated electric fields. Fields are sorted by decreasing vibrational frequency of CCSD(T) results (black curve), so may not correspond to the same indexing as CO results. The CCSD(T) gas phase vibrational frequency is shown for reference (dashed line). The charge models are based on AIM (red) and DMA (green) atomic multipole moments.

VI. Simulations of CO in Ice

The CO absorption band in ices has been characterized using spectroscopic techniques[50−52] for different CO/water fractions and at different temperatures.[50,53,54] These studies have established that the details of composition and thermodynamic conditions influence the shape, width, and splitting of the CO absorption band from which conclusions about physicochemical properties of the interstellar and circumstellar regions, including star-forming regions and dark clouds, can be drawn.

Here an idealized system, CO in hexagonal ice, is considered to compare the performance of different electrostatic models. For the interpretation of the spectra it should be noted that the spectral shift depends on more factors than in the previous model calculations. One of these factors is the sampling which may be different for the various electrostatic models, because

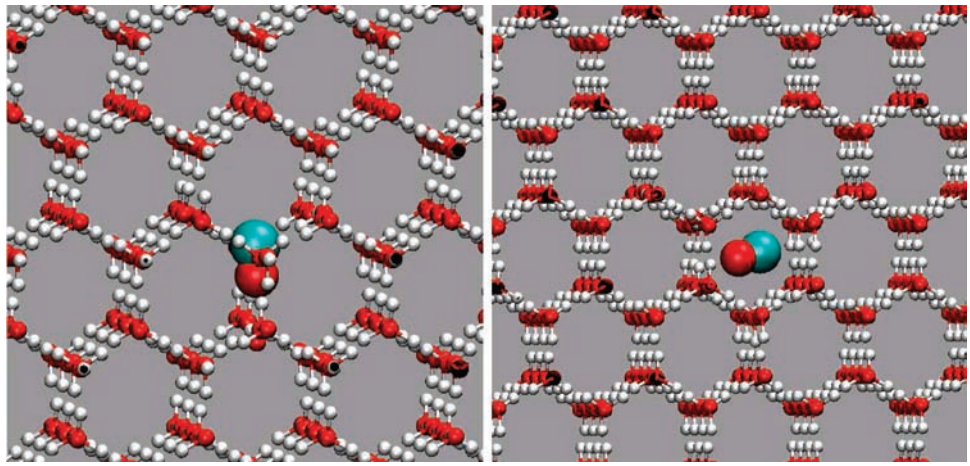

Figure 7. Initial structures for the MD simulations of CO in ice. The structural CO is shown on the left-hand side and the interstitial on the right-hand side.

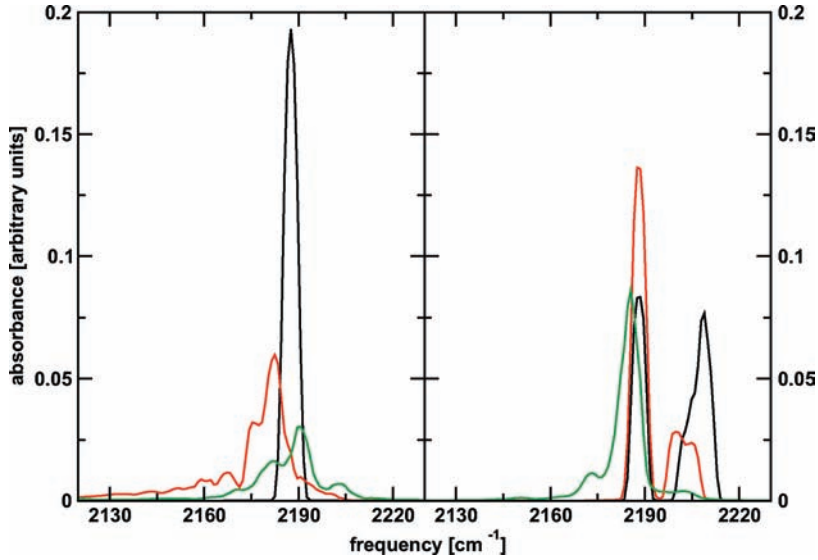

Figure 8. Average spectra from simulations of CO in hexagonal ice using different multipolar charge models. The panel on the left side shows spectra for the structural CO positions, the right side spectra for the interstitial CO position. Black color represents the simple point charge model, red color the model C′, and green color the AIM model.

different electrostatic models favor slightly different positions and orientations in the ice lattice. It is expected that the differences are largest between the simple point charge model and the three multipole models. Another factor to take into account is the structural transformation of the ice structure due to the presence of the CO molecule. This effect is expected to be stronger for stronger electrostatic interactions.

For each model, seven trajectories 100 ps in length are evaluated at 20 K for both the structural (Figure 7, left) and the interstitial position (Figure 7, right) in the ice. The average spectra from simulations with point charges, Model C' and the AIM model are shown in Figure 8. During the simulations the CO molecules move ≈1 to 3 Å away from their initial position and the structure of the surrounding ice slightly adjusts due to the presence of the CO molecule. Furthermore, the CO molecule can change its orientation, which is observed mainly for the interstitial position.

For interstitial positions, two frequency bands are found for the simple point charge model and model C′ (Figure 8 right panel). The two bands result from different orientations of the CO inside the ice which are rotated with respect to the initial orientation. The intensities of the two bands are different for the point charge model and model C′ because the molecular multipole moments differ and therefore the preferential orientation changes. The similarity of the shifts for the two models is probably related to the fact that the interactions with the surrounding ice are dominated by van der Waals interactions. The AIM model shows one broad band, red shifted with respect to the other two models. This is due to the fact that it has a larger vibrational response to the electric field of the ice and therefore also leads to larger structural changes in its environment.

For the structural position, the simple point charge model shows no shift with respect to the free CO frequency and no broadening of the frequency band. This is due to the fact that it interacts very weakly with the ice. The other two models have broader spectra and the bands are red-shifted. The broadening is larger for the AIM model due to its stronger interaction with the ice. The spectra for model C are very similar to the spectra for model C′. The only difference is the broadening, which is somewhat larger than for model C′, but not as broad as for the AIM model.

The results are qualitatively consistent with the findings for CO in the inhomogeneous field (see above), where models C and C′ are similar to each other and the AIM model shows the largest shifts. For CO in hexagonal ice the larger shifts for the AIM model can be related to the large broadening of the spectra,

whereas for the simple point charge model the absence of broadening and vibrational shift is related to its minimal interaction with the inhomogeneous field.

In conclusion, for the three models differences in the spectroscopy are found which can be related to the detail of the multipole model. However, as MD simulations using different models also lead to different sampling of phase space, vibrational spectra from MD trajectories cannot be solely attributed to the response of a molecule to an applied field (as characterized by static calculations involving point charges). The structural ice position, for example, exhibits a number of nearby metastable states that appear to be occupied differently by different charge models. Sampling of phase space and magnitude of the vibrational response are therefore two different effects that cannot generally be separated in MD simulations. It is also emphasized that the results for CO in hexagonal ice should not be directly compared with experimental data, as done, e.g., in ref 14, because the water model used here is useful for conceptual studies but not suitable for quantitative ones.

VII. Conclusions

In this work we investigated vibrational frequency shifts of small probe molecules represented by multipolar force fields in inhomogeneous electric fields. By use of DFT calculations, it was shown that the vibrational shift of CO in an inhomogeneous electric field can deviate strongly from the behavior in a uniform field. This suggests that calculations or measurements performed in uniform fields may not be suitable to interpret measurements carried out in heterogeneous environments.

For CO, simple charge models and different multipolar models have been tested to evaluate their influence on characterizing vibrational shifts in a series of randomly generated, inhomogeneous electric fields. It is demonstrated that representing charge distributions by a superposition of point charges is typically not sufficient for a realistic description of the vibrational response. Atomic multipole moments provide a compact and more realistic representation, with small differences between models arising from the partitioning method used to decompose the electron density.[15−17] Additionally, the three-point fluctuating charge model[10] approach has been shown to yield reliable vibrational frequency shifts, although the lack of accurate higher molecular multipole moments can affect details of the sampling in MD simulations. It should be noted that mixed quantum/classical mechanical (QM/MM) studies have been used in the past to study vibrational spectroscopy.[55−58] In principle, such an approach retains multipole moments to arbitrarily high orders (limited only by the basis sets used). In practice, however, the applicability of QM/MM is limited due to the considerably larger computational cost to sample configuration space. The approach pursued in the present work can be viewed as "QM/MM", where the quantum part is treated by a DMA which can, in principle, be made arbitrarily accurate. However, there are also cases where improvements to the electrostatic interactions only are not sufficient to better capture the vibrational spectroscopy, as shown in recent work on CO ligated to Mb.[59,60]

Calculations for H_2 in an external inhomogeneous field have revealed similarities to CO, due to interactions between the higher multipole moments and higher field derivatives. The substantial shifts calculated at the CCSD(T) level of theory—despite the lack of a molecular dipole moment—demonstrate the importance of effects due to the inhomogeneous field when interpreting frequency shifts in heterogeneous molecular environments. The lack of a responsive term to account for bond weakening as a function of the applied field in the case of H_2 means that no vibrational frequency shift occurs upon interaction of the multipole models with an applied uniform electric field. Neglect of this bond weakening term also leads to poorer performance of the multipole models in heterogeneous fields than was the case for CO.

Finally, MD simulations of CO trapped in hexagonal ice demonstrate that the findings of the model Stark shift calculations can be related to the shifts found in a realistic system. The interpretation of the spectra is more involved, since also sampling of different positions and orientations as well as transformations of the surrounding structure have to be taken into account.

Acknowledgment. The authors gratefully acknowledge financial support from the Swiss National Science Foundation under Grant 200021-117810.

References and Notes

(1) Boxer, S. G. *J. Phys. Chem. B* **2009**, *113*, 2972.
(2) Webb, L. J.; Boxer, S. G. *Biochemistry* **2008**, *47*, 1588.
(3) Plattner, N.; Meuwly, M. *Biophys. J.* **2008**, *94*, 2505.
(4) Lewell, X. Q.; Hillier, I. H.; Field, M. J.; Morris, J. J.; Taylor, P. J. *J. Chem. Soc., Faraday Trans. 2* **1988**, *84*, 893.
(5) Lefebvre-Brion, H.; Field, R. W. *The Spectra and Dynamics of Diatomic Molecules*; Elsevier Academic Press: Paris, 2004.
(6) Ansari, A.; Berendzen, J.; Braunstein, D.; Cowen, B. R.; Frauenfelder, H.; Kyung Hong, M.; Iben, I. E. T.; Johnson, J. B.; Ormos, P.; Sauke, T. B.; et al. *Biophys. Chem.* **1987**, *26*, 337.
(7) Phillips, G.; Teodoro, M.; Li, T.; Smith, B.; Olson, J. *J. Phys. Chem. B* **1999**, *103*, 8817.
(8) Rovira, C.; Schulze, B.; Eichinger, M.; Evanseck, J. D.; Parrinello, M. *Biophys. J.* **2001**, *81*, 435.
(9) Lim, M.; Jackson, T. A.; Anfinrud, P. A. *J. Chem. Phys.* **1995**, *102*, 4355.
(10) Nutt, D. R.; Meuwly, M. *Biophys. J.* **2003**, *85*, 3612.
(11) Johnson, J.; Lamb, D.; Frauenfelder, H.; Muller, J.; McMahon, B.; Nienhaus, G.; Young, R. D. *Biophys. J.* **1996**, *71*, 1563.
(12) Suydam, I. T.; Snow, C. D.; Pande, V. S.; Boxer, S. G. *Science* **2006**, *313*, 200.
(13) McQuarrie, D. A. *Statistical Mechanics*; Harper's Chemistry Series; Harper and Row: New York, 1976.
(14) Plattner, N.; Meuwly, M. *ChemPhysChem* **2008**, *9*, 1271.
(15) Bader, R. F. W., *Atoms in molecules—Aquantum theory*; Oxford University Press: Oxford, 1990.
(16) Popelier, P. L. A. *Atoms in Molecules. An Introduction*; Pearson Education: London, U.K., 2000.
(17) Stone, A. J.; Alderton, M. *Mol. Phys.* **1985**, *56*, 1047.
(18) Hush, N. S.; Williams, M. L. *J. Mol. Spectrosc.* **1974**, *50*, 349.
(19) Hush, N. S.; Reimers, J. R. *J. Phys. Chem.* **1995**, *99*, 15798.
(20) Andrews, S. S.; Boxer, S. G. *J. Phys. Chem. A* **2002**, *106*, 469.
(21) Bishop, D. M. *Rev. Mod. Phys.* **1990**, *62*, 343.
(22) Stone, A. J., *The Theory of Intermolecular Forces*; Clarendon Press, Oxford, 1996.
(23) Liem, S. Y.; Popelier, P. L. A. *J. Chem. Phys.* **2003**, *8*, 4560.
(24) Leslie, M. *Mol. Phys.* **2008**, *106*, 1567.
(25) Shaik, M.; Devereux, M.; Popelier, P. L. A. *Mol. Phys.* **2008**, *12*, 1495.
(26) Becke, A. D. *J. Chem. Phys.* **1993**, *98*, 5648.
(27) Stephens, P. J.; Devlin, F. J.; Chabalowski, C. F.; Frisch, M. J. *J. Phys. Chem.* **1994**, *98*, 11623.
(28) Frisch, M. J.; Trucks, G. W.; Schlegel, H. B.; Scuseria, G. E.; Robb, M. A.; Cheeseman, J. R.; Montgomery, J. A., Jr.; Vreven, T.; Kudin, K. N.; Burant, J. C.; Millam, J. M.; Iyengar, S. S.; Tomasi, J.; Barone, V.; Mennucci, B.; Cossi, M.; Scalmani, G.; Rega, N.; Petersson, G. A.; Nakatsuji, H.; Hada, M.; Ehara, M.; Toyota, K.; Fukuda, R.; Hasegawa, J.; Ishida, M.; Nakajima, T.; Honda, Y.; Kitao, O.; Nakai, H.; Klene, M.; Li, X.; Knox, J. E.; Hratchian, H. P.; Cross, J. B.; Adamo, C.; Jaramillo, J.; Gomperts, R.; Stratmann, R. E.; Yazyev, O.; Austin, A. J.; Cammi, R.; Pomelli, C.; Ochterski, J. W.; Ayala, P. Y.; Morokuma, K.; Voth, G. A.; Salvador, P.; Dannenberg, J. J.; Zakrzewski, V. G.; Dapprich, S.; Daniels, A. D.; Strain, M. C.; Farkas, O.; Malick, D. K.; Rabuck, A. D.; Raghavachari, K.; Foresman, J. B.; Ortiz, J. V.; Cui, Q.; Baboul, A. G.; Clifford, S.; Cioslowski, J.; Stefanov, B. B.; Liu, G.; Liashenko, A.; Piskorz, P.; Komaromi, I.; Martin, R. L.; Fox, D. J.; Keith, T.; Al-Laham, M. A.; Peng, C. Y.; Nanayakkara, A.; Challacombe, M.; Gill, P. M. W.; Johnson, B.; Chen, W.; Wong, M. W.; Gonzalez, C.; Pople, J. A. *Gaussian 03, Revision C.01*; Gaussian, Inc.: Wallingford, CT, 2004.

(29) MacKerell, A. D., Jr.; Bashford, D.; Bellott, M.; Dunbrack, R. L., Jr.; Evanseck, J. D.; Field, M. J.; Fischer, S.; Gao, J.; Guo, H.; Ha, S.; et al. *J. Phys. Chem. B* **1998**, *102*, 3586.
(30) Stone, A. J. *J. Chem. Theory Comput.* **2005**, *1*, 1128.
(31) Popelier, P. L. A. *Morphy98*; UMIST: Manchester, England, 1998.
(32) Le Roy, R. J. *Chemical Physics Research Report*; CP-555R; University of Waterloo: Waterloo, ON, 1996.
(33) Jorgensen, W. L.; Chandrasekhar, J. D.; Madura, J. D.; Impey, R. W.; Klein, M. L. *J. Chem. Phys.* **1983**, *79*, 926.
(34) Brooks, B. R.; Bruccoleri, R. E.; Olafson, B. D.; States, D. J.; Swaminathan, S.; Karplus, M. *J. Comput. Chem.* **1983**, *4*, 187.
(35) Berendsen, H. J. C.; Postma, J. P. M.; van Gunsteren, W. F.; DiNola, A.; Haak, J. R. *J. Chem. Phys.* **1984**, *81*, 3684.
(36) van Gunsteren, W.; Berendsen, H. *Mol. Phys.* **1977**, *34*, 1311.
(37) Huffaker, J. N. *J. Chem. Phys.* **1976**, *64*, 3175.
(38) Huffaker, J. N. *J. Chem. Phys.* **1976**, *64*, 4564.
(39) Allen, M. P. Tildesley, D. J. *Computer Simulation of Liquids*; Clarendon Press: Oxford, 1987.
(40) Park, E. S.; Andrews, S. S.; Hu, R. B.; Boxer, S. G. *J. Phys. Chem. B* **1999**, *103*, 9813.
(41) Maroulis, G. *J. Phys. Chem.* **1996**, *100*, 13466.
(42) Maroulis, G. *Chem. Phys. Lett.* **2001**, *334*, 214.
(43) Roco, J. M. M.; Calvo Hernández, A.; Velasco, S. *J. Chem. Phys.* **1995**, *103*, 9161.
(44) Roco, J. M. M.; Medina, A.; Calvo Hernndez, A.; Velasco, S. *J. Chem. Phys.* **1995**, *103*, 9175.
(45) Popelier, P. L. A.; Joubert, L.; Kosov, D. S. *J. Phys. Chem. A* **2001**, *105*, 8254.
(46) Joubert, L.; Popelier, P. L. A. *Phys. Chem. Chem. Phys.* **2002**, *4*, 4353.
(47) Joubert, L.; Popelier, P. L. A. *Mol. Phys.* **2002**, *100*, 3357.
(48) Buckingham, A. D.; Coriani, S.; Rizzo, A. *Theor. Chem. Acc.* **2007**, *117*, 969.
(49) Bishop, D. M.; Cybulski, S. M. *J. Chem. Phys.* **1994**, *101*, 2180.
(50) Palumbo, M. E.; Strazzulla, G. *Astron. Astrophys.* **1993**, *269*, 568.
(51) Gerakines, P. A.; Schutte, W. A.; Greenberg, J. M.; van Dishoeck, E. F. *Astron. Astrophys.* **1995**, *296*, 810.
(52) Collings, M. P.; Dever, J. W.; Fraser, H. J.; McCoustra, M. R. S.; Williams, D. *Astrophys. J.* **2003**, *583*, 1058.
(53) Sandford, S. A.; Allamandola, L. J. *Icarus* **1988**, *76*, 201.
(54) Schmitt, B.; Greenberg, J. M.; Grim, R. J. A. *Astrophys. J.* **1989**, *340*, L33.
(55) Nutt, D. R.; Meuwly, M. *Proc. Natl. Acad. Sci.U.S.A.* **2004**, *101*, 5998.
(56) Meuwly, M. *ChemPhysChem* **2006**, *10*, 2061.
(57) Sauer, J.; Dobler, J. *ChemPhysChem* **2005**, *6*, 1706.
(58) Meuwly, M.; Karplus, M. *J. Chem. Phys.* **2002**, *116*, 2572.
(59) Devereux, M.; Meuwly, M. *Biophys. J.* **2009**, *96*, 4363.
(60) Devereux, M.; Meuwly, M. *J. Phys. Chem. B*, in press.

JP903954T